THE JOURNAL OF NAVIGATION (2004), **57**, 103–116. © The Royal Institute of Navigation
DOI: 10.1017/S0373463303002509 Printed in the United Kingdom

Robust Trajectory Planning for Target Following Vision-based Autonomous Land Vehicle Guidance

Ching-Heng Ku

(*National Center for High-performance Computing, Taiwan*)

Wen-Hsiang Tsai

(*National Chiao Tung University*)

We propose a robust trajectory planning method for vision-based autonomous land vehicle (ALV) guidance by target following using a visual field model. The proposed trajectory planning method aims to guide the ALV to achieve the goal that the targeted person will always appear in the image. It is found in this study that the goal can be achieved if three visual contact constraints in the visual field model are satisfied. The first constraint postulates that the target has appeared in the image. The second constraint asks that the vehicle head at the next position points straight towards to the target's current position. The third constraint sets bounds between the next position of the ALV and the current position of the target. A formula for the trajectory of the vehicle that satisfies the second visual contact constraint is derived. The steps for generating a speed and a turn angle of the ALV for real-time navigation are described as a trajectory-planning algorithm. Finally, the approach is tested on a real ALV and successful navigation sessions confirm the feasibility and the robustness of the approach.

KEY WORDS

1. Trajectory-planning. 2. Land vehicle guidance. 3. Visual field model.

1. INTRODUCTION. In recent years, many approaches to autonomous land vehicle (ALV) guidance in indoor or outdoor environments have been developed. These methods depend on the use of extracted features such as lines [3][4], corners [5][6], models [7][8], roads [11][12], cars [13][14], persons [15–17], or special landmarks [9][10]. In this paper we study the guidance of a vision-based ALV by following the target of a walking person. When a vision-based ALV navigates by following a target, that target has to be detected on the image captured by a camera. Our method for person detection from images was introduced in detail in [1]. After the relative position of the target to the ALV is calculated, a trajectory for the ALV guidance needs to be generated to obtain the turn angle for the front wheels of the ALV. Some trajectory planning approaches [18–19] have been proposed. These methods do not generate a robust trajectory for a vision-based vehicle following a person. The goal of this study is to propose a robust trajectory planning

https://doi.org/10.1017/S0373463303002509 Published online by Cambridge University Press

method to guide the ALV so that the target always appears in the captured image. In this study, we focus on the steps of trajectory planning and following.

Our proposed robust trajectory planning method is based on the visual field model and three visual contact constraints. The visual field model includes the proposed visible area and target-bounded area. When the visible area of the ALV totally covers the target-bounded area, the target's next position can be confirmed to appear in the captured image. Using this property we find that if three visual contact constraints in the visual field model are satisfied, we can achieve the goal that the target always appears in the image. Hence, a formula for the trajectory of the vehicle will be derived. Robust navigation will be achieved when the ALV follows the trajectory. In addition, in order to implement the proposed method in a real ALV, the maximum speed and the maximum turn angle of the ALV are considered. We propose two theorems to specify some conditions for the derived trajectory. Accordingly, a proper turn angle of the front wheels of the ALV can be calculated. The steps for generating the trajectory of the ALV in real time are described as a trajectory-planning algorithm. By executing the algorithm, the ALV can keep visual contact with the target at any time and keep within a certain range of the target.

2. PROPOSED VISUAL FIELD MODEL AND VISUAL CONTACT CONSTRAINTS.

In our visual field model, we consider the visual field of the camera and the possible positions of the target walking in front of the ALV. A camera mounted on the ALV to capture the person's image and its visual field is bounded by the visual angle of the camera. Because the ALV cannot move with the abrupt directional changes of a person, capturing the target's image at one instant does not guarantee a successful image capture of the target at the next moment. Hence, all possible positions of the person at the next instant have to be included in the visual field of the camera. This condition will be formulated by the visual contact constraints proposed in Section 2.2. The definition of the visual field model is described in Section 2.1.

2.1. *Definition of Proposed Visual Field Model.*

In this study, the direction of the optical axis of the camera is adjusted to be the same as that of the ALV head. As illustrated in Figure 1, the proposed visual field model is composed of the visible area of the camera, the interior of the triangle, whilst the interior of the circle is defined as the person-bounded target area. The camera possesses a constant visual angle (the angle 2α), whose magnitude depends on the lens of the camera. In this study, the visual angle of the camera was assumed to be known. Hence, the visible area of the current ALV position B is defined to be the area bounded by the left and the right boundary lines which form the visual angle 2α of the camera, as shown in Figure 1. The person-bounded area is defined as the area that covers all possible positions of the person at the next time interval. Here, a unit time is defined as the time interval between two image samplings. A circle is defined to cover all possible positions of the person at any time instant. The circle is just the person-bounded area of the person position P at speed v for time t.

2.2. *Proposed Visual Contact Constraints.*

In order to keep the person within the visible area, the area must totally cover the person-bounded area at any time. An illustration of the positions B and P of the ALV and the person, respectively, at two time instants are shown in Figure 2, where the visible areas of B_i and B_{i+1} totally

https://doi.org/10.1017/S0373463303002509 Published online by Cambridge University Press

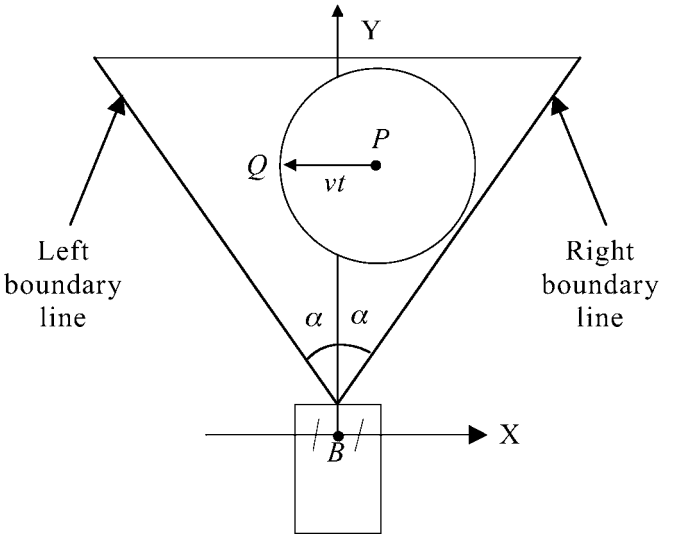


Figure 1. Illustration of the visible area and the person-bounded area.

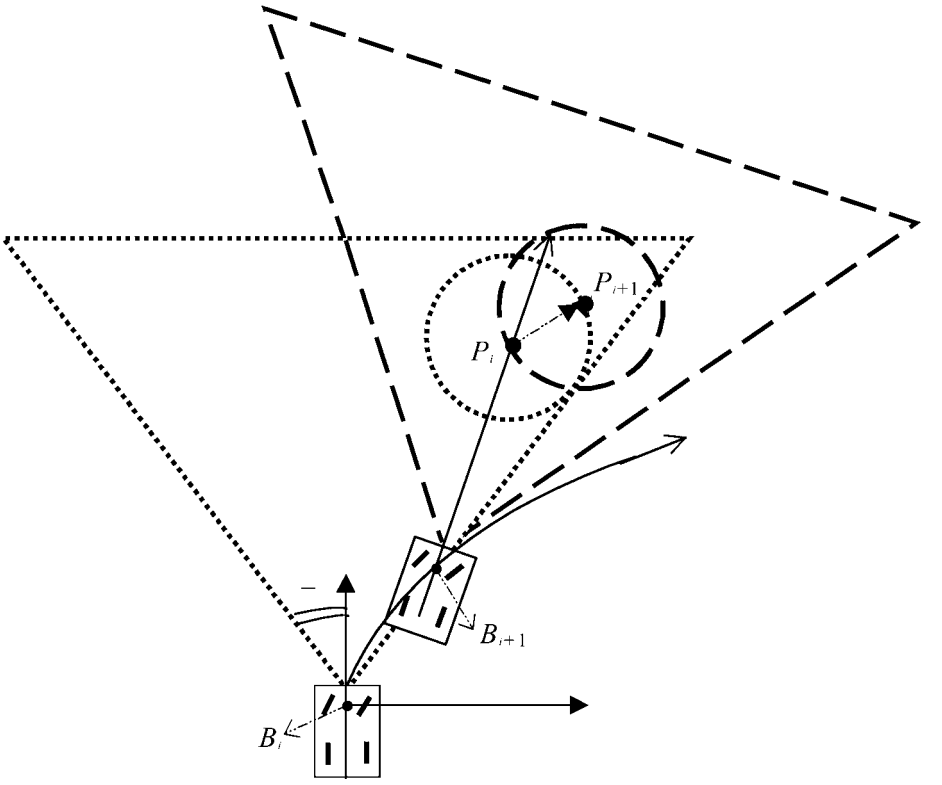


Figure 2. Illustration of the ALV (B) and the target position (P) at two time instants.

https://doi.org/10.1017/S0373463303002509 Published online by Cambridge University Press

cover the person-bounded areas of P_i and P_{i+1}, respectively. Accordingly, the three proposed visual contact constraints are formulated to guarantee that the target always appears in the image at any time instant:

$$A(B_i,\ P_i) \leqslant \alpha \tag{1}$$

$$A(B_{i+1},\ P_i) = 0 \tag{2}$$

$$d_1 \leqslant D(B_{i+1},\ P_i) \leqslant d_2 \tag{3}$$

where B_i and B_{i+1} represent the current and the next positions of the vehicle, respectively, P_i represents the current position of the target, A denotes the angle between the direction of the vehicle head and that from the origin of the vehicle coordinate system to the target position P_i, D is the distance between the vehicle and the target, α is a half of the visual angle, and d_1 and d_2 are two pre-selected limiting distances.

The first constraint in (1) is a precondition for the others and guarantees that the target's current position P_i is located in the visible area. The second and the third constraints in (2) and (3) describe two intended relations between B_{i+1} and P_i. The second constraint says that the person's current position P_i is desirably straight in front of the vehicle head (i.e. the camera direction) at the next position B_{i+1} of the vehicle so that the angle $A(B_{i+1}, P_i)$ is zero. This constraint can be achieved by the proposed trajectory derived in the next section. Constraint (3) says that the distance between B_{i+1} and P_i must be bounded in a certain range defined by d_1 and d_2 (described in detail in Section 3.2) so that the person-bounded area of P_i can be totally covered by the visible area of B_{i+1}. When these three constraints are satisfied, the person's next position P_{i+1} can be guaranteed to appear in the visible area of B_{i+1}.

3. TRAJECTORY DERIVATION.

3.1. *Trajectory Derivation to Satisfy the Second Visual Contact Constraint.* In this section, we derive a trajectory to satisfy the second visual contact constraint. More specifically, we derive a proper turn angle δ under a given speed V to generate a circular trajectory for the vehicle to follow. A detailed model for the kinematic trajectory of a vehicle was introduced in [20], from which the trajectory and the position of the vehicle at the next time instant can be obtained. The model for an automobile with front and rear tyres [2] is shown in Figure 3. The centre position between the two front wheels is taken as the origin of the vehicle coordinate system. This assumption is helpful to derive a simple formula for the trajectory.

The desired kinematic trajectory for the vehicle to follow is taken to be a circular curve. The position B in Figure 3 is assumed to be a certain point on the circular path with coordinates x and y. The values of x and y can be expressed as functions, the results are [20]:

$$\begin{aligned} x = P\cos u &= R\sqrt{2(1-\cos r)}\cos\left(\frac{\pi}{2}-\delta-\frac{r}{2}\right) \\ &= \frac{d}{\sin\delta}\sqrt{2\left(1-\cos\frac{S\sin\delta}{d}\right)}\cos\left(\frac{\pi}{2}-\delta-\frac{S\sin\delta}{2d}\right), \end{aligned} \tag{4}$$

https://doi.org/10.1017/S0373463303002509 Published online by Cambridge University Press

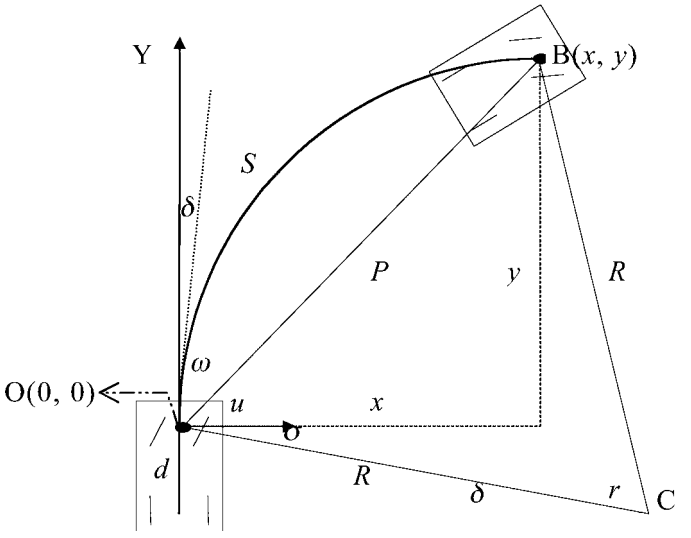


Figure 3. Analysis of the path S on which the vehicle navigates from O to B by turning an angle of δ.

$$y = P\sin u = R\sqrt{2(1-\cos r)}\sin\left(\frac{\pi}{2}-\delta-\frac{r}{2}\right)$$
$$= \frac{d}{\sin\delta}\sqrt{2\left(1-\cos\frac{S\sin\delta}{d}\right)}\sin\left(\frac{\pi}{2}-\delta-\frac{S\sin\delta}{2d}\right), \quad (5)$$

where P is the straight distance from the origin O to point B, u is the angle between the x-axis and the vector $\boldsymbol{OB}$ and $S = Vt$.

Hence, x and y can be modified as functions of δ and V to be:

$$x = f(\delta, V) \quad \text{and} \quad y = g(\delta, V) \quad (6)\,(7)$$

Accordingly, as shown in Figure 4, when the front wheels of the vehicle turns δ degrees and arrives at location B by travelling a circular curve, the direction vector $\boldsymbol{v}_2$ of the front wheels will be that of the tangent of the curve. Let the vector from the location B to the person's position P be $\boldsymbol{v}_1$ and let the angle between $\boldsymbol{v}_1$ and $\boldsymbol{v}_2$ be θ. The value of δ denotes the angle between the direction of the vehicle head and that of the front wheels at the next time instant. When the second visual contact constraint is satisfied, the following constraint should be true:

$$h(\theta, \delta) = \theta - \delta = 0 \quad (8)$$

The derivation of the angle of θ can be elaborated as:

$$\theta = \cos^{-1}\left(\frac{v_1 \,.\, v_2}{|v_1| \,.\, |v_2|}\right)$$
$$= \cos^{-1}\left(\frac{(x_1-x)\,.\,(d+y)+(y_1-y)\,.\,(d\cot\delta-x)}{\sqrt{(x_1-x)^2+(y_1-y)^2}\,.\,\sqrt{(d+y)^2+(d\cot\delta-x)^2}}\right), \quad (9)$$

https://doi.org/10.1017/S0373463303002509 Published online by Cambridge University Press

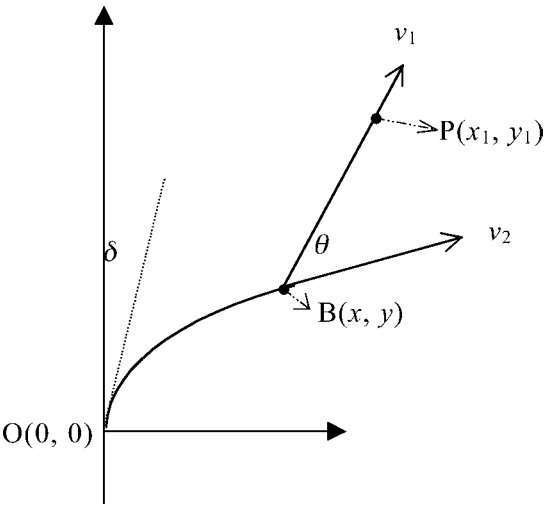


Figure 4. Illustration of the relationship between the vehicle position B and the target position P.

where:

$$v_2 = (d + y,\ d\cot\delta - x) \tag{10}$$

Because x and y are functions of δ and V, the angle θ can be formulated in terms of the variables δ and V as a function G. Hence, the function h in Equation (8) can be modified as a function H as follows:

$$H(\delta,\ V) = h(\theta,\ \delta) = G(\delta,\ V) - \delta = 0 \tag{11}$$

The approach to obtain the speed V of the vehicle is introduced in Section 5. When the function (11) is satisfied according to a calculated δ and a given V, the position of the vehicle at the next time instant will satisfy the second visual contact constraint and the circular curve S will be a proper navigation trajectory.

3.2. *Limiting Distances to Satisfy the Third Visual Contact Constraint*. As shown in Figure 5, d_1 is the nearest distance and d_2 the furthest distance between the target's current and the vehicle's next position. These two values can be calculated according to the relation between the visible area and the person-bounded area. Because the target's next position must be located inside the person-bounded area, the distance $v_p t$ that the person walks in a unit time must be smaller than the radius of the person-bounded area. Hence, the value of the distance d_1 can be calculated as:

$$d_1 = v_p t / \sin\alpha \tag{12}$$

As shown in Figure 5(b), when the farthest boundary of the visible area is the tangent of the person-bounded area, the distance d_2 can be calculated accordingly. Assume that the distance from the farthest boundary of the visible area to the position of the vehicle is y_{max}. Then, the farthest distance d_2 can be taken to be:

$$d_2 = y_{max} - v_p t \tag{13}$$

The value y_{max} in (13) may be derived in terms of the maximum speed V_{max} of the vehicle, the maximum turn angle A_{max} of the front wheels, and the visual angle 2α of

https://doi.org/10.1017/S0373463303002509 Published online by Cambridge University Press

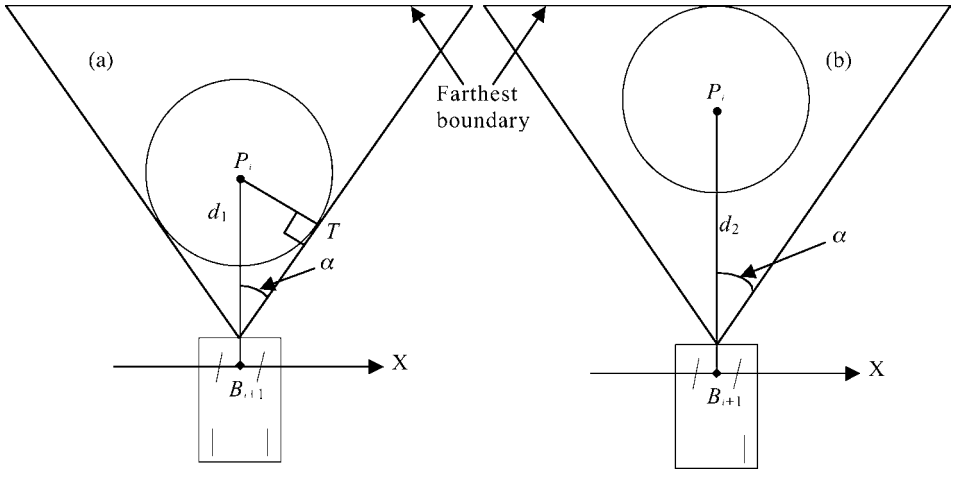


Figure 5. Illustration of the boundaries in the third constraint. (a) Lower boundary d_1. (b) Upper boundary d_2.

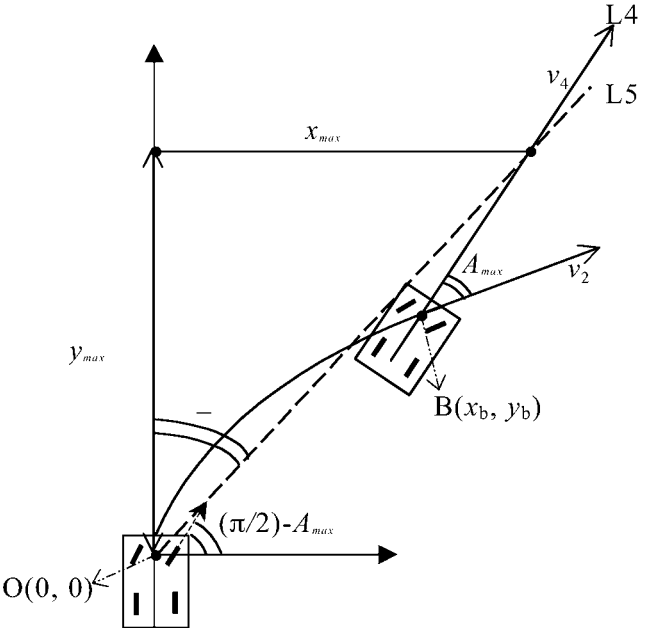


Figure 6. The maximum distance Y_{max} is derived from the maximum vehicle speed V_{max}, the front wheel maximum turn angle A_{max} and the camera visual angle 2α.

the camera. After the ALV navigates using the speed V_{max} and the turn angle A_{max} in a unit time, the ALV arrives at position B. The direction vector $\boldsymbol{v_2}$ of the front wheels at position B, as shown in Figure 6, can be derived as:

$$\boldsymbol{v_2} = (d + y_b,\ d\cot(A_{max}) - x_b), \tag{14}$$

where x_b and y_b are the coordinates of the vehicle at position B and d is the vehicle length. The coordinates x_b and y_b may be obtained in terms of A_{max} and V_{max} from

https://doi.org/10.1017/S0373463303002509 Published online by Cambridge University Press

Equations (6) and (7) as two functions:

$$x_b = f(A_{max},\ V_{max}), \quad y_b = f(A_{max},\ V_{max}) \tag{15)(16}$$

After the direction vector v_2 of the front wheels is obtained from (14), the direction vector v_4 of the vehicle head can be obtained using the condition that the angle between v_2 and v_4 is A_{max}, shown as:

$$v_4 = (x_4,\ y_4) = v_2 \cdot \begin{bmatrix} \cos A_{max} & \sin A_{max} \\ -\sin A_{max} & \cos A_{max} \end{bmatrix}. \tag{17}$$

Now, the equation of the line passing through the point B and with the vector v_4 as its direction can be written as:

$$L4:\ \frac{y_4}{x_4}x + \left(y_b - \frac{y_4}{x_4}x_b\right) - y = 0. \tag{18}$$

The angle between the right boundary line L5, that passes through the origin of the VCS, of the visible area, and the direction of the vehicle head is α. Hence, the line equation of L5 is:

$$L5:\ x(\cot\alpha) - y = 0. \tag{19}$$

According to Equations (18) and (19), the coordinates x_{max} and y_{max} of the intersection point of L4 and L5 can be obtained as:

$$x_{max} = \frac{y_b x_4 - y_4 x_b}{(\cot\alpha)x_4 - y_4} \quad \text{and} \quad y_{max} = \frac{(\cot\alpha)(y_b x_4 - y_4 x_b)}{(\cot\alpha)x_4 - y_4} \tag{20}$$

According to (12), (13) and (20), the third constraint can be rewritten as:

$$d_1 = v_p t / \sin\alpha \leqslant D(B_{i+1},\ P_i) \leqslant \frac{(\cot\alpha)(y_b x_4 - y_4 x_b)}{(\cot\alpha)x_4 - y_4} - v_p t = d_2 \tag{21}$$

By Equation (21), there exist some conditions when the third visual contact constraints are correctly achieved in the successive navigation. There will be two theorems proposed in the next section.

4. ANALYSIS OF THE VISUAL CONTACT CONSTRAINTS.

In this section, we propose two theorems from an analysis of the visual contact constraints by considering the maximum speed and the maximum turn angle of the ALV in the navigation. The first theorem specifies the condition for the second visual contact constraint. The second theorem specifies the condition for all visual contact constraints such that the person at the next position must appear in the image that is captured from the next vehicle position. First, we define two regions, Region 1 and Region 2, which exist in the visible area. As illustrated in Figure 7, the area bounded by the Y-axis of the VCS and the line L4 is named the direction-covered area. All positions in the direction-covered area will be directly ahead of the vehicle head during the time t in which the ALV navigates from the position O to position B. The intersection area of the right-hand side of the visible area and the direction-covered area is defined as a position-candidate area. There exists an obvious condition that the distance between the vehicle and the target needs to be greater than a navigation distance $V_i t$ of the vehicle, where V_i is the current speed

https://doi.org/10.1017/S0373463303002509 Published online by Cambridge University Press

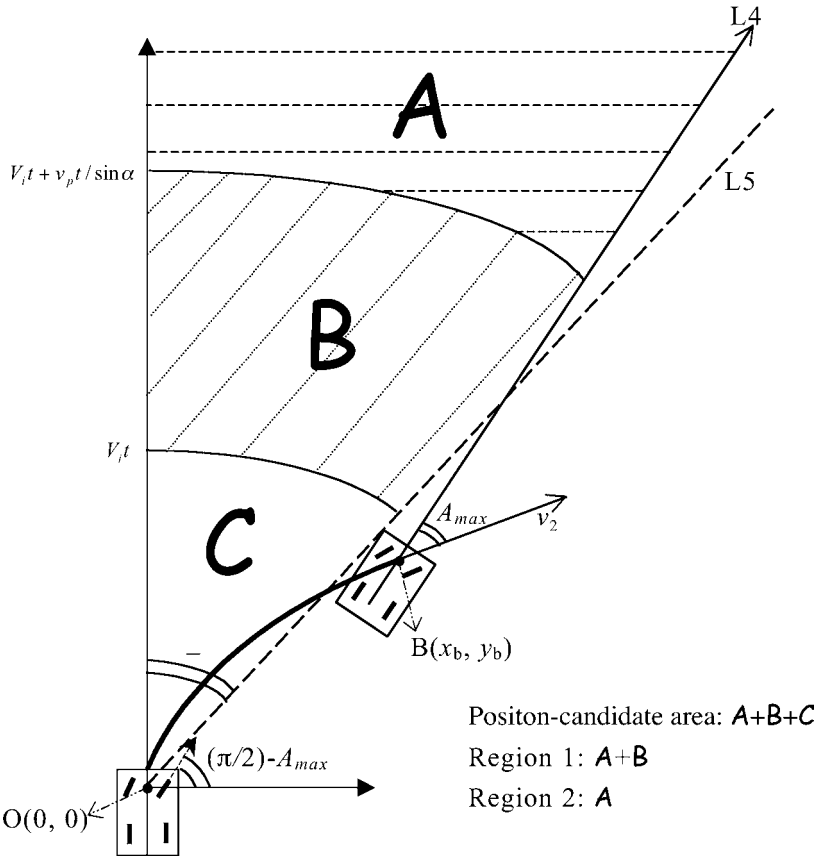


Figure 7. Illustration of Regions 1 and 2.

of the vehicle. Hence, we define Region 1 as the area that contains all the positions in the position-candidate area whose distance to the origin of the VCS is larger than $V_i t$. All positions in Region 1 can satisfy the second visual contact constraint. This statement will be introduced in Theorem 1. Furthermore, we define Region 2 as the area which contains all the positions in the position-candidate area whose distance to the origin of the VCS is greater than $V_i t + d_1$, where d_1 is the lower boundary of the distance in the third visual contact constraint and its value is $v_p t/\sin\alpha$. If the target's position is in Region 2, the person at the next position must appear in the captured image at the next position of the vehicle. This statement will be introduced in Theorem 2.

Theorem 1. If the person's current position P_i is located in Region 1, there must exist a next vehicle position B_{i+1} such that the second visual contact constraint $A(B_{i+1}, P_i) = 0$ is true.

The following corollary considers a more specific condition in Theorem 1. This condition represents a situation that the right-hand side of the visible area is totally covered by the direction-covered area, as shown in Figure 8. Hence, the position-candidate area is substituted by the right-hand side of the visible area so that the position inside Region 1 must be located in the view of the camera.

https://doi.org/10.1017/S0373463303002509 Published online by Cambridge University Press

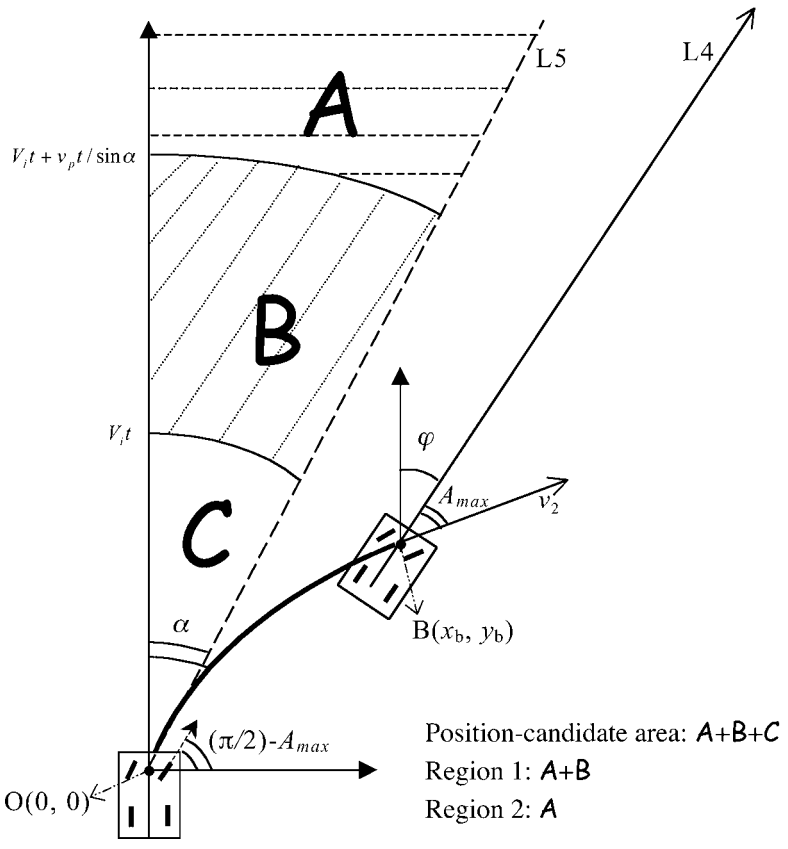


Figure 8. Illustration of α and φ.

Corollary 1. If the angle φ between the direction of the vehicle head at the position B and that at the position O is larger than the angle α, the person's current position P_i is located inside the visible area of B_i (i.e. $A(B_i, P_i) \leqslant \alpha$), and the distance between the vehicle and the person is larger than $V_i t$ (i.e. $V_i t \leqslant D(B_i, P_i)$), then there must exist a next vehicle position B_{i+1} such that the second visual contact constraint $A(B_{i+1}, P_i) = 0$ is true.

The following theorem specifies the condition for the next position of the person to always appear in the view of the camera at the next position of the vehicle.

Theorem 2. If the person's current position P_i is located in Region 2, there must exist a next vehicle position B_{i+1} such that the next person position P_{i+1} satisfies the inequality $A(B_{i+1}, P_{i+1}) \leqslant \alpha$.

The following corollary considers a specific situation that the angle α is smaller than the angle φ in Theorem 2.

Corollary 2. If the angle φ between the direction of the vehicle head at position B and that at O is larger than the angle α, the person's current P_i is located inside the visible area of B_i (i.e. $A(B_i, P_i) \leqslant \alpha$), and the distance between the vehicle and the person is larger than $V_i t + v_p t / \sin\alpha$ (i.e. $V_i t + v_p t / \sin\alpha \leqslant D(B_i, P_i)$), then there must

https://doi.org/10.1017/S0373463303002509 Published online by Cambridge University Press

exist a next vehicle position B_{i+1} such that the next person position P_{i+1} satisfies the inequality $A(B_{i+1}, P_{i+1}) \leqslant \alpha$.

The two theorems specify the conditions for the derived ALV trajectory and the desired trajectory planning method in the real navigation. Using the condition in Theorem 2, an upper boundary of the speed of the vehicle can be derived. This boundary is used in the proposed algorithm described in the next section so that robust navigation can be achieved.

5. PROPOSED TRAJECTORY PLANNING ALGORITHM.

The control parameters, turn angle and vehicle speed, can be derived for the ALV navigation from the following proposed trajectory planning algorithm:

- Step 1. If the person P_i is in the image, calculate the target's speed v_p and coordinates (x_1, y_1), and continue. Otherwise, stop the vehicle and go to Step 1.
- Step 2. Calculate the distance D between the target's position P_i and the position B_i of the vehicle.
- Step 3. Calculate the lower boundary V_l of the speed by solving the following equation for V_l:

$$H(A_{max}, V_l) = G(A_{max}, V_l) - A_{max} = 0. \tag{22}$$

  where A_{max} is a pre-set constant. If the distance between B_i and P_i is smaller than $V_l t$, i.e. if $D(B_i, P_i) \leqslant V_l t$, stop the vehicle and go to Step 1. Otherwise, continue.
- Step 4. According to Corollary 2, the upper boundary V_u of the speed can be calculated by:

$$V_u = \frac{D(B_i, P_i) - v_p t / \sin\alpha}{t} = \frac{D(B_i, P_i)}{t} - \frac{v_p}{\sin\alpha}. \tag{23}$$

- Step 5. Assign the speed V_i of the vehicle according to the person's speed v_p, the upper boundary V_u and the lower boundary V_l using the following rule:
  If $V_u \leqslant V_l$ is true, then assign V_l to V_i; otherwise, execute one of the following three assignments:
  if $v_p \leqslant V_l$ is true, then assign V_l to V_i;
  if $V_l \leqslant v_p \leqslant V_u$ is true, then assign v_p to V_i;
  if $v_p \geqslant V_u$ is true, then assign V_u to V_i.
- Step 6. Calculate the turn angle δ of the vehicle according to the given speed V_i of the vehicle. The angle δ is calculated by iteration to satisfy the following equation:

$$H(\delta, V_i) = G(\delta, V_i) - \delta = 0. \tag{24}$$

- Step 7. Send the control parameters of V_i and δ to the vehicle.
- Step 8. Go to Step 1.

This algorithm achieves the goal of robust real time navigation.

6. EXPERIMENTAL RESULTS.

Our method has been tested by steering an ALV to follow a walking person and is illustrated in Figure 9. In our experiments the ALV is 40 cm wide and 120 cm long, the length d between the front and

https://doi.org/10.1017/S0373463303002509 Published online by Cambridge University Press



Figure 9. The vehicle is guided automatically to follow a target walking in front.



(a) (b)

Figure 10. Illustration of the effect of applying the trajectory-planning algorithm. (a) shows that the target's position is close to the left boundary line of the camera. (b) shows the result of applying the algorithm.



Figure 11. A sequence of experimental images in the corridor of an indoor environment.

rear wheels is 82 cm. The maximum speed V_{max} of the vehicle is 80 cm/sec and the front wheels have a maximum turn angle A_{max} of 30 degrees to the right or left. The unit time t between two sampling instants is one sec. The lens and the visual angle

https://doi.org/10.1017/S0373463303002509 Published online by Cambridge University Press

2α of the camera are 8 mm and 50 degrees, respectively. The structure of the vehicle system is introduced in detail in [20].

Figure 10 shows some images from the ALV in the corridor using the trajectory-planning algorithm. The target's position is close to the left boundary line of the camera. In this particular manoeuvre, the algorithm modified the speed of the vehicle to 14·60 cm/sec and the turn angle of the front wheels was -35 degrees; the vehicle robustly kept visual contact with the person. An example of a sequence of experimental images in a real indoor environment is shown in Figure 11 where the robustness of the derived trajectory keeping the ALV in visual contact at reasonable range from the target as he moves along a corridor and turns through a 90 degree corner is demonstrated.

7. CONCLUSIONS. In this study, a robust trajectory planning method has been proposed so that a moving target will always appear in the captured image when followed by the ALV. The goal is achieved when three visual contact constraints in the visual field model are satisfied. We have derived a trajectory for the ALV to follow which satisfies the second visual contact constraint. In addition, the maximum speed and the maximum turn angle of the ALV were also considered. Two theorems have been derived to specify conditions for the derived trajectory and the proposed trajectory planning method. By using the condition of the second theorem, an upper boundary of the speed of the ALV is obtained. The steps for generating the control parameter of the robust navigation are proposed as a trajectory-planning algorithm. The approach was been tested by experiments on a real ALV and successful navigation sessions confirm the feasibility and robustness of the approach.

REFERENCES

[1] C. H. Ku and W. H. Tsai, "Smooth Autonomous Land Vehicle Navigation in Indoor Environments by Person Following Using Sequential Pattern Recognition, Fuzzy Speed Control and Computer Vision Techniques," *Proceedings of the Joint Conference of the Fifth International Conference on Automation Technology and 1998 International Conference of Production Research* (*Asia Meeting*), Grand Hotel, Taipei, Taiwan, Republic of China, pp. 115, 20–22 July, 1998.

[2] R. M. Murray and S. S. Sastry, "Nonholonomic motion planning: steering using sinusoids," *IEEE Transaction on Automatic Control*, vol. 38, No. 5, pp. 700–716, 1993.

[3] M. S. Chang, P. Y. Ku, L. L. Wang, and W. H. Tsai, "Indoor autonomous land vehicle guidance by line following using computer vision techniques," *Proceedings of 1989 Workshop on Computer Vision, Graphics, and Image Processing*, Taipei, Taiwan, Republic of China, pp. 135–144, 1989.

[4] B. Matthews, M. Ruthemeyer, D. Perdue, and E. L. Hall, "Line following for a mobile robot," *Proceedings of the SPIE – The International Society for Optical Engineering*, Vol. 2588, pp. 610–617, 1995.

[5] W. J. Ke and W. H. Tsai, "Indoor autonomous land vehicle guidance by corner tracking using computer vision," *Proceedings of 1991 Workshop on Computer Vision, Graphics and Image Processing*, Tainan, Taiwan, Republic of China, pp. 133–139, 1991.

[6] Y. M. Su and W. H. Tsai, "Autonomous land vehicle guidance for navigation in buildings by computer vision, radio, and photoelectric sensing techniques," *Journal of the Chinese Institute of Engineers*, Vol. 17, No. 1, pp. 63–73, 1994.

[7] H. I. Christensen, N. O. Kirkeby, S. Kristensen, L. Knudsen, and E. Granum, "Model-driven vision for indoor navigation," *Robotics and Autonomous Systems*, Vol. 12, No. 3–4, pp. 199–207, 1994.

[8] L. L. Wang, P. Y. Ku, and W. H. Tsai, "Model-based guidance on the longest common subsequence algorithm for indoor autonomous vehicle navigation using computer vision," *Automation in Construction*, Vol. 2, No. 2, pp. 123–137, 1993.

https://doi.org/10.1017/S0373463303002509 Published online by Cambridge University Press

[9] T. Fukuda, S. Ito, N. Oota, F. Arai, Y. Abe, K. Tanaka, and Y. Tanaka, "Navigation system based on ceiling landmark recognition for autonomous mobile robot," *Proceedings of the IECON. International Conference on Industrial Electronics, Control, and Instrumentation*, Vol. 3, pp. 1466–1471, 1993.

[10] Gilg and G. Schmidt, "Landmark-oriented visual navigation of a mobile robot," *IEEE Transactions on Industrial Electronics*, Vol. 41, No. 4, pp. 392–397, 1994.

[11] C. Thrope, M. H. Hebert, T. Kanade, and S. A. Shafer, "Vision and navigation for Carnegie-Mellon NAVLAB," *IEEE Transactions on Pattern Analysis and Machine Intelligence*, Vol. 10, No. 3, pp. 362–373, 1988.

[12] J. D. Crisman and C. E. Thorpe, "SCARF: A color vision system that tracks roads and intersections," *IEEE Transactions on Robotics and Automation*, Vol. 9, No. 1, pp. 49–58, 1993.

[13] K. I. Kim, S. Y. Oh, S. W. Kim, H. Jeong, J. H. Han, C. N. Lee, B. S. Kim, and C. S. Kim, "An autonomous land vehicle PRV II: progresses and performance enhancement", *Proceedings of the Intelligent Vehicles '95. Symposium*, Detroit, MI, U.S.A., pp. 264–269, 1995.

[14] M. Schwarzinger, T. Zielke, D. Noll, M. Brauckmann, and W. von Seelen, "Vision-based car-following: detection, tracking, and identification", *IEEE Intelligent Vehicles Symposium*, pp. 24–29, 1992.

[15] K. Matsuda, M. Kamihira, M. Onchi, and T. Furukawa, "Design and implementation of tracking control system of autonomous mobile robot with multiple sensors," *Reports of the Faculty of Science and Engineering, Saga University*, Vol. 24, No. 1, pp. 73–82, 1995.

[16] U. D. Hanebeck and G. Schmidt, "A new high performance multisonar system for fast mobile robots," *IROS. Proceedings of the IEEE/RSJ/GI International Conference on Intelligent Robots and Systems. Advanced Robotic Systems and the Real World*, Vol. 3, pp. 1853–1860, 1994.

[17] H. Mori and M. Sano, "A guide dog robot Harunobu-5 – following a person," *Proceedings IROS. IEEE/RSJ International Workshop on Intelligent Robots and Systems. Intelligence for Mechanical Systems*, Vol. 1, pp. 397–402, 1991.

[18] V. F. Munoz and A. Ollero, "Smooth trajectory planning method for mobile robots," *Proceedings of Conference on Computational Engineering in Systems Applications*, pp. 700–705, Lille, France, 9–12 July, 1996.

[19] Z. Shiller and W. Serate, "Trajectory planning of tracked vehicles," *Journal of Dynamic Systems Measurement and Control-Transactions of the ASME*, Vol. 117, No. 4, pp. 619–624, 1995.

[20] C. H. Ku and W. H. Tsai, "Obstacle Avoidance for Autonomous Land Vehicle Navigation in Indoor Environments by Quadratic Classifier," *IEEE Transactions on Systems, man, and Cybernetics*, Vol. 29: Part B, No. 3, June 1999.

https://doi.org/10.1017/S0373463303002509 Published online by Cambridge University Press